JOURNAL OF VIROLOGY, Aug. 2009, p. 8254–8258 Vol. 83, No. 16
0022-538X/09/$08.00+0 doi:10.1128/JVI.00580-09

Suppression of Human Immunodeficiency Virus Type 1 (HIV-1) Viremia with Reverse Transcriptase and Integrase Inhibitors, CD4$^+$ T-Cell Recovery, and Viral Rebound upon Interruption of Therapy in a New Model for HIV Treatment in the Humanized Rag2$^{-/-}\gamma_c^{-/-}$ Mouse$^{\nabla}$†

Shailesh K. Choudhary,[1]* Naser L. Rezk,[2] William L. Ince,[3] Manzoor Cheema,[1] Liguo Zhang,[4] Lishan Su,[3,4] Ronald Swanstrom,[3] Angela D. M. Kashuba,[2] and David M. Margolis[1,4,5]*

Department of Medicine,[1] School of Pharmacy,[2] Curriculum in Genetics and Molecular Biology,[3] and Departments of Microbiology and Immunology[4] and Epidemiology,[5] University of North Carolina, Chapel Hill, North Carolina 27599

Received 20 March 2009/Accepted 23 May 2009

A small animal model that reproduces human immunodeficiency virus type 1 (HIV-1) pathogenesis may allow modeling of new therapeutic strategies in ways not approachable in mononuclear cell culture. We find that, as in humans, combination antiretroviral therapy (ART) in humanized (hu-) Rag2$^{-/-}\gamma_c^{-/-}$ mice allows suppression of viremia below the limits of detection and recovery of CD4$^+$ cells, while interruption of ART results in viral rebound and renewed loss of CD4$^+$ T cells. Failure of ART in infected mice is associated with the appearance of drug resistance mutations. The hu-Rag2$^{-/-}\gamma_c^{-/-}$ mouse may therefore facilitate testing of novel approaches to HIV replication and persistence.

Combination antiretroviral therapy (ART) is best tested in a complete biological system but is difficult to test in nonhuman primates (NHPs) (1). NHPs infected with a chimeric simian-human immunodeficiency virus (SHIV) encoding human immunodeficiency virus type 1 (HIV-1) reverse transcriptase (RT-SHIV) can be used to test reverse transcriptase inhibitors; however, NHP resources are limited (2, 18). BLT (bone marrow liver thymic) mice have been successfully used to model antiretroviral preexposure prophylaxis, but have not yet been used to model ART (7).

Humanized (hu-) Rag2$^{-/-}\gamma_c^{-/-}$ mice, reconstituted with human CD34$^+$ hematopoietic stem cells (HSCs), display engraftment of T, B, myeloid, and NK cells in both central and peripheral lymphoid organs (3, 22, 23). Substantial plasma viremia and systemic depletion of human CD4$^+$ T cells follow infection with CCR5- or CXCR4-tropic HIV (4, 23).

The nucleoside/nucleotide reverse transcriptase inhibitors (NRTIs) tenofovir (TFV) disoproxil fumarate (TDF) and emtricitabine (FTC) have long elimination half-lives and are widely used as part of daily ART (10). The strand transfer inhibitor (InSTI) raltegravir is being studied for use in initial therapy for HIV with TDF/FTC (17), and InSTI L-870812 is potent in the SHIV-infected macaque (13). Due to the difficulty of reliable long-term dosing of protease inhibitors and nonnucleoside RTIs in mice, we chose to study a dual NRTI-InSTI regimen in hu-Rag2$^{-/-}\gamma_c^{-/-}$ mice.

hu-Rag2$^{-/-}\gamma_c^{-/-}$ mice suffered depletion of hu-CD4$^+$ T cells following HIV-1 infection, a prompt decline in plasma viremia after the initiation of ART, and recovery of hu-CD4$^+$ T cells following therapy. In some treated mice, viremia rebounded after initial suppression, in association with RTI and InSTI resistance mutations. Recapitulating ART in humans, hu-Rag2$^{-/-}\gamma_c^{-/-}$ mice are a promising model for testing ART and novel therapeutic strategies.

ART dosing and PK studies in Rag2$^{-/-}\gamma_c^{-/-}$ mice. Rag2$^{-/-}\gamma_c^{-/-}$ mice were dosed with single intraperitoneal injection of L-870812, FTC, and TFV at 20, 60, and 50 mg/kg body weight, respectively. Doses were based on previous studies in mice and NHPs (13, 18, 20). The concentrations of drugs were measured simultaneously using a multiplex high-performance liquid chromatography method with UV detection (19). Serum was subjected to solid-phase extraction using BOND ELUT C_{18} columns. Intestinal tissue (IT) samples were subjected to solid-phase extraction after homogenization. Analytes were separated using an Atlantis dC_{18} analytical column (Waters Corp., Milford, MA) and a gradient elution. Calibration curves for both matrices ranged from 5 to 1,000 ng/ml for TFV and L-870812 and from 10 to 1,000 ng/ml for FTC. Interday and intraday coefficients of variation across the range of concentrations were less than 13%.

Table 1 shows the pharmacokinetic (PK) parameters of each antiretroviral in blood plasma and IT over a 24-h

* Corresponding authors. Mailing address for S. K Choudhary: University of North Carolina at Chapel Hill, 3206 Michael Hooker Research Ctr., CB#7435, Chapel Hill, NC 27599-7435. Phone: (919) 966-6389. Fax: (919) 966-0584. E-mail: schoudha@med.unc.edu. Mailing address for D. M. Margolis: University of North Carolina at Chapel Hill, 3302 Michael Hooker Research Ctr., CB#7435, Chapel Hill, NC 27599-7435. Phone: (919) 966-6388. Fax: (919) 966-0584. E-mail: dmargo@med.unc.edu.

† Supplemental material for this article may be found at http://jvi.asm.org/.

$^{\nabla}$ Published ahead of print on 3 June 2009.

TABLE 1. Plasma and tissue PK parameters for TFV, FTC, and L-870812[a]

Sample type and drug	C_{max}[b]	C_{24}[b]	AUC_{0-24}[c]	$t_{1/2}$ (h)
Mouse plasma				
TFV	3,660 (262–9,936)	38 (1–13)	12,122 (7,631–85,570)	5 (2–8)
FTC	18,641 (670–22,784)	46 (16–69)	49,514 (27,055–149,002)	4 (3–5)
L-870812	4,996 (330–13,720)	8 (0.5–10)	15,095 (2,878–65,128)	3 (2–4)
Mouse IT				
TFV	39 (7–88)	4 (2–31)	352 (87–513)	10 (7–12)
FTC	31 (8–51)	5 (1–15)	175 (54–191)	17 (4–36)
L-870812	31 (8–67)	0.4 (0.1–2)	87 (48–236)	4 (2–8)
Human plasma				
TFV	292	53	2,650	15
FTC	1,650	71	11,000	10

[a] Median values are presented, with ranges in parentheses. Mouse PK parameters were compared with human data as described in reference 5.
[b] Values are ng/ml for mouse and human plasma and ng/mg for IT.
[c] Values are h · ng/ml for mouse and human plasma and h · ng/mg for IT.

period in Rag2$^{-/-}\gamma_c^{-/-}$ mice and their comparison to human plasma (6). The PK of TFV, FTC, and L-870812 were evaluated by noncompartmental methods using WinNonlin (5.1; Pharsight, Mountain View, CA). The terminal elimination rate constant (λ_z) was estimated by linear regression of the terminal portion of the log-transformed concentration versus time curve using at least the last three data points in the terminal elimination phase. The terminal half-life ($t_{1/2}$) was calculated as $\ln(2)/\lambda_z$. The maximum observed concentration (C_{max}) was obtained directly from the concentration-time profile. The area under the curve (AUC) from time 0 to the last measured concentration at 24 h (C_{24}), AUC_{0-24}, was determined using the trapezoidal rule with linear-up/log-down interpolation.

Serum concentrations of TFV and FTC dosed intraperitoneally in mice were similar to C_{24}s achieved in humans when dosed orally (Table 1 and Fig. 1). The median $t_{1/2}$s of TFV and FTC in IT were 10 h and 17 h, respectively, and were two- to fourfold higher than in serum. This indicates a continued presence of drug in cells, despite a decline in plasma drug concentration. In contrast to human metabolism, enterohepatic recirculation was observed for all three drugs between 6 and 12 h. Although enterohepatic recirculation can alter the PK of drugs by increasing exposure, reducing clearance, and extending half-life, this property allows drug dosing in mice at a frequency used in humans to obtain similar concentrations at C_{24}.

The serum concentration of L-870812 at 12 h was well above the 95% inhibitory concentration (250 to 350 nM), but declined to 21 nM at 24 h (13). InSTI, however, acts in a nonreversible manner, and so antiviral effect may persist after plasma concentrations decline (11). Total concentrations of parent drugs measured in IT were also sufficient to suppress viremia, suggesting that once-daily antiviral dosing could be sufficient to control HIV-1 infection in hu-Rag2$^{-/-}\gamma_c^{-/-}$ mice.

hu-Rag2$^{-/-}\gamma_c^{-/-}$ mice are engrafted with long-lived memory CD4$^+$ T cells. hu-Rag2$^{-/-}\gamma_c^{-/-}$ mice were created by transplanting human fetal liver-derived CD34$^+$ cells (0.5×10^6 to 1×10^6) into the livers of newborn conditioned Rag$^{-/-}\gamma_c^{-/-}$ mice as previously described (5, 22, 23), with modifications. Briefly, CD34$^+$ HSC were cultured overnight in RPMI 1640 medium containing interleukin-3 (IL-3), IL-6, and stem cell factor (1, 1, and 2 μg/ml, respectively) prior to injection. We found stable engraftment of hu-CD45$^+$ T cells in peripheral blood (PB) and lymphoid tissue (Fig. 2A). More than 50% of the hu-CD4$^+$ T cells in PB, lymph node (LN), spleen, and IT were CD45RO$^+$ memory cells, a site of persistent HIV-1 in-

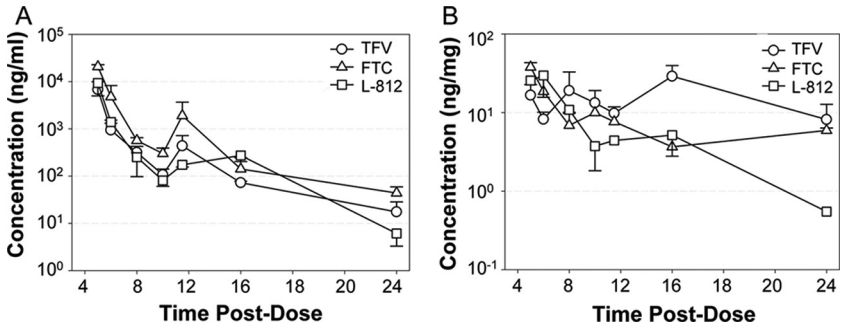

FIG. 1. Pharmacokinetics of ART in Rag2$^{-/-}\gamma_c^{-/-}$ mice. Mice were dosed with FTC, TFV, and L-870812 (L-812) at 60, 50 and 20 mg/kg body weight by single intraperitoneal injection. Serum and gastrointestinal tissue samples from ileum and rectum were collected and frozen at −80°C until analysis. As the PK profiles were similar for ileum and rectal regions of IT, data were combined. The data shown are the mean concentration ± standard error of the single-dose PK profile of FTC, TFV, and L-870812 over a 24-h period in serum (A) and IT (B) of mice after combined intraperitoneal injection. $n = 3$ for serum, and $n = 6$ for tissue.

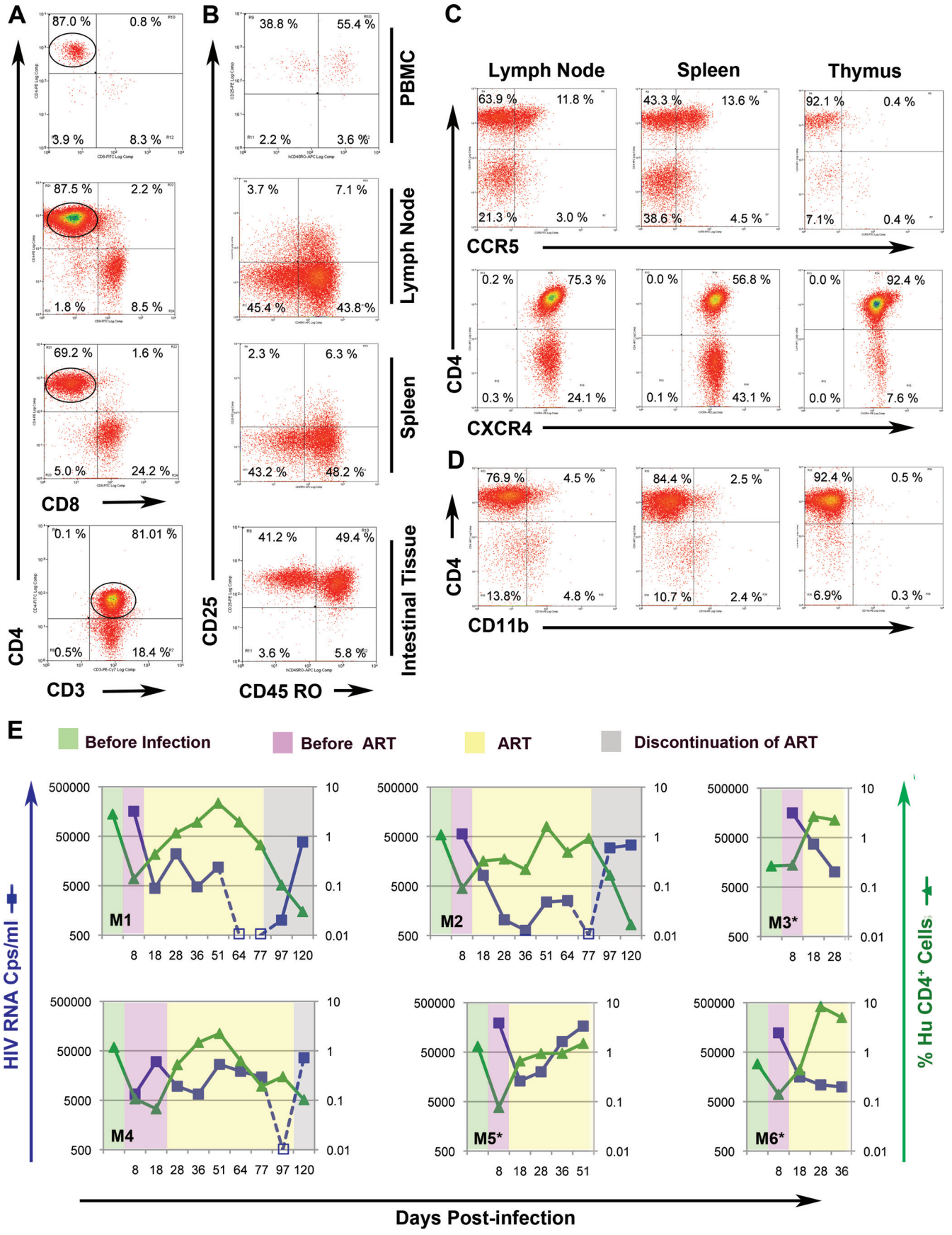
A
87.0 %
0.8 %
3.9 %
8.3 %
87.5 %
2.2 %
1.8 %
8.5 %
69.2 %
1.6 %
5.0 %
24.2 %
0.1 %
81.01 %
0.5%
18.4 %
CD4
CD8
CD3
B
38.8 %
55.4 %
2.2 %
3.6 %
3.7 %
7.1 %
45.4 %
43.8 %
2.3 %
6.3 %
43.2 %
48.2 %
41.2 %
49.4 %
3.6 %
5.8 %
PBMC
Lymph Node
Spleen
Intestinal Tissue
CD25
CD45 RO
C
Lymph Node
Spleen
Thymus
63.9 %
11.8 %
21.3 %
3.0 %
43.3 %
13.6 %
38.6 %
4.5 %
92.1 %
0.4 %
7.1%
0.4 %
CCR5
0.2 %
75.3 %
0.3 %
24.1 %
0.0 %
56.8 %
0.1 %
43.1 %
0.0 %
92.4 %
0.0 %
7.6 %
CD4
CXCR4
D
76.9 %
4.5 %
13.8%
4.8 %
84.4 %
2.5 %
10.7 %
2.4 %
92.4 %
0.5 %
6.9%
0.3 %
CD4
CD11b
E
Before Infection
Before ART
ART
Discontinuation of ART
HIV RNA Cps/ml
% Hu CD4+ Cells
M1
M2
M3*
M4
M5*
M6*
500000
50000
5000
500
10
1
0.1
0.01
8 18 28 36 51 64 77 97 120
Days Post-infection

fection. The majority of CD45RO$^+$ CD4$^+$ T cells residing in the spleen and LN lacked the activation markers CD25 (Fig. 2B), CD69, and HLA-DR (data not shown). In contrast, CD45RO$^+$ CD4$^+$ cells in blood and IT expressed CD25 but lacked HLA-DR (data now shown), indicating partial activation status. We recovered human cells from IT by collagenase D digestion (21) of the entire intestine, including ileum and rectum, followed by Ficoll-Paque enrichment of human lymphocytes. We observed more than 5% hu-CD45$^+$ cells in two of six mice, which was infrequent compared to that in BLT mice (21). Our results are consistent with the findings of Berges et al. (4), who similarly reconstitute mice with cytokine-treated CD34$^+$ HSCs, but in contrast to those of Hofer et al. (14).

We noted that even hu-Rag2$^{-/-}\gamma_c{}^{-/-}$ mice with poor circulating human cell engraftment (1 to 5%) had higher engraftment in lymphoid organs; 75% of cells in thymus and LN were hu-CD45$^+$. Engrafted hu-CD4$^+$ T cells expressed both CCR5 and CXCR4 coreceptors (Fig. 2C), and therefore could be infected by either CCR5- or CXCR4-tropic virus. Major lymphoid organs also contained CD11b$^+$ myeloid/NK cells (Fig. 2D) and CD14$^+$ macrophages (data not shown). hu-Rag2$^{-/-}\gamma_c{}^{-/-}$ mice therefore possess the critical cells necessary to model HIV-1 infection and ART.

Novel ART in HIV-1-infected hu-Rag2$^{-/-}\gamma_c{}^{-/-}$ mice allows viral suppression and recovery of hu-CD4$^+$ T cells. We infected six mice intravenously with CCR5-tropic HIV-1 JR-CSF and monitored plasma viremia and hu-CD4$^+$ T-cell percentage over a 4-month period (Fig. 2E). Plasma viremia was assayed using the Abbott RealTime reverse transcription (RT)-PCR automated m2000 system (Abbott, Des Plaines, IL). All mice became infected, and a decline in hu-CD4$^+$ T cells was observed following peak viremia. Due to high levels of viremia and rapid and profound hu-CD4 depletion seen in preliminary studies (see Fig. S1 in the supplemental material), ART was initiated at 8 days postinfection in all mice except M4, in which ART was initiated at 18 days postinfection. Infected mice were treated daily by intraperitoneal injection. Mice that received prompt ART had a decline in plasma viremia of 0.6 to 1.5 log in 10 days of treatment. In contrast, viral load increased in M4, in which ART was delayed and viral suppression lagged by the approximately the same length of time. Untreated mice maintained high viral loads (see Fig S1 in the supplemental material).

Suppression of viremia following ART allowed recovery of hu-CD4$^+$ T cells in the PB. Interestingly, we observed that CD4$^+$ T-cell rebound occurred in M1 and M4 even when viremia was only partially suppressed. We noted an increase in percentage of hu-CD4$^+$ cells relative to hu-CD45$^+$ cells (see Fig. S2 in the supplemental material), which indicates that in response to CD4$^+$ depletion, a selective proliferation of T cells occurred. An increase in CD4$^+$ T-cell number despite an increase in viremia for a shorter time period was also observed by another group in this model (3, 5). It is likely that partial suppression of viremia by ART enabled the response of T-cell homeostasis mechanisms.

Continuation of ART resulted in viral suppression below the limit of detection at 7 to 9 weeks of treatment in three mice (M1, M2, and M4). We observed a typical initial rapid decline in plasma viremia after the start of ART followed by a gradual decline. Discontinuation of ART after suppression of viremia in M1 and M2 resulted in viral rebound and renewed loss of hu-CD4$^+$ T cells. Mice M3 and M6 also showed initial viral suppression and increases in circulating hu-CD4$^+$ cells; however, evaluation was incomplete due to the death of the mice. Incidental mortality is sometimes seen in this humanized mouse model, and drug toxicity is not likely to be causal: longer periods of ART (3.5 months) were well tolerated in other animals.

In M5, following an initial decline, viremia increased rapidly. M4 exhibited a delayed response to ART. We sequenced the viral polymerase (*pol*) gene to seek evidence of drug resistance mutations. Amplicons were generated from limiting dilution PCR using the ABI BigDye Terminator system. We detected drug resistance mutations associated with NRTIs (K65R) (16) and InSTI (M154I) (12) in M4 after rebound and M5 at failure (Table 2). M5 exhibited another mutation associated with raltegravir resistance (E92Q) (15). The significance of mutation in the conserved DD(35)E motif (E152I) of integrase in relation to drug resistance is not known (8, 9).

In summary, combination ART in HIV-1-infected hu-Rag2$^{-/-}\gamma_c{}^{-/-}$ mice recapitulates many aspects of ART in humans. Suppression of viremia, CD4$^+$ T-cell maintenance and recovery, viral persistence, and the emergence of drug-resistant virus are observed in this model. Model systems such as this one may allow the testing of novel approaches to the

FIG. 2. hu-CD4$^+$ T-cell reconstitution, infection, and novel antiretroviral therapy in hu-Rag2$^{-/-}\gamma_c{}^{-/-}$ mice. (A) T-cell reconstitution at 20 weeks postengraftment. Live cells were defined based on their forward and side scatter and single cells based on forward scatter height and area. Single, live cells were subsequently gated on the hu-CD45$^+$/mouse CD45 and hu-CD3$^+$ population. (B) Memory hu-CD4$^+$ T cells reconstitute in blood and tissue. Human T cells gated on the CD4$^+$ population (circled) were analyzed for memory marker CD45RO and activation marker CD25. PBMC, peripheral blood mononuclear cells. (C) hu-CD4$^+$ T-cell expression of CCR5 and CXCR4. (D) hu-CD11b$^+$ cells are detected in several lymphoid tissues. (E) Suppression of plasma viremia and recovery of hu-CD4$^+$ T cells in individual hu-Rag2$^{-/-}\gamma_c{}^{-/-}$ mice. Animals were infected with JRCSF (25 ng p24/mouse) and treated with L-870812, TFV, and FTC at 20, 50, and 60 mg/kg/daily, respectively. Blue lines and squares show plasma viremia, while green lines and triangles show CD4$^+$ percentages, both drawn on a logarithmic scale. The percentage of hu-CD4$^+$ T cells represents the percentage of this cell population in total peripheral blood mononuclear cells obtained from mouse blood. The percentage of hu-CD4$^+$ T cells = % hu-CD45$^+$/mouse CD45$^-$ cells $\times$ (% CD3$^+$ cells gated on hu-CD45$^+$ cells/100) $\times$ (% CD4$^+$ cells gated on hu-CD45$^+$ CD3$^+$/100). Due to the small available volume of mouse plasma, dilution is required, and so the limit of assay detection of viral RNA is $<$500 copies (Cps)/ml. Shading indicates time prior to infection (green), following infection (purple), after initiation of ART (yellow), and following discontinuation of ART (gray). TFV- and L-870812-related mutations were detected in plasma of M4 and M5 upon failure of therapy or rebound. Experiments terminated by death of the mouse are indicated by asterisks.

TABLE 2. Appearance of Pol amino acid substitutions associated with drug resistance during ART

Mouse	No. of amino acid substitutions/amplicons sequenced												
	Reverse transcriptase									Integrase (to amino acid 261)			
	E6K	E53K	K65R	Y115F	R199K	G262E	E302K	D364N	E432K	D55N	E92Q	E152K	M154I
M4	0/10	1/10	6/10	1/10	0/10	0/10	0/10	1/10	0/10	0/10	0/10	0/10	4/10
M5	1/11	0/11	11/11	0/11	1/11	1/11	1/11	0/11	1/11	1/11	1/11	2/11	2/11

treatment of HIV infection beyond standard ART, such as gene therapy or eradication approaches.

We thank the Central Institute for Experimental Animals, Kawasaki, Japan, for providing Rag2$^{-/-}\gamma_c^{-/-}$ mice. Thanks are also due to G. Kovalev, D Cothran, D. Parker, A. James, J. Nelson, and S. Fiscus for technical advice and support; N. Archin and K. Keedy for critically reading the manuscript; and the University of North Carolina (UNC) Center for AIDS Research (CFAR; NIH award P30 AI50410) Virology, Pharmacology, and Immunology Cores and the Division of Laboratory Animal Medicine for assistance. We also thank Gilead Sciences (Foster City, CA) and the Merck Research Laboratory (West Point, PA) for providing RTIs and integrase inhibitor, respectively.

This work was supported by a UNC-CFAR developmental grant (P30 AI50410), and National Institute of Health grants R21 AI 081613-01A1 to S.K.C and R37 AI44667 to R.S. W.L.I. received support from NIH training grants T32 AI07419 and T32 GM07092.

REFERENCES

1. **Ambrose, Z., V. Boltz, S. Palmer, J. M. Coffin, S. H. Hughes, and V. N. KewalRamani.** 2004. In vitro characterization of a simian immunodeficiency virus-human immunodeficiency virus (HIV) chimera expressing HIV type 1 reverse transcriptase to study antiviral resistance in pigtail macaques. J. Virol. **78:**13553–13561.
2. **Ambrose, Z., S. Palmer, V. F. Boltz, M. Kearney, K. Larsen, P. Polacino, L. Flanary, K. Oswald, M. Piatak, Jr., J. Smedley, W. Shao, N. Bischofberger, F. Maldarelli, J. T. Kimata, J. W. Mellors, S. L. Hu, J. M. Coffin, J. D. Lifson, and V. N. KewalRamani.** 2007. Suppression of viremia and evolution of human immunodeficiency virus type 1 drug resistance in a macaque model for antiretroviral therapy. J. Virol. **81:**12145–12155.
3. **Baenziger, S., R. Tussiwand, E. Schlaepfer, L. Mazzucchelli, M. Heikenwalder, M. O. Kurrer, S. Behnke, J. Frey, A Oxenius, H Joller, A Aguzzi, M. G. Manz, and R. F. Speck.** 2006. Disseminated and sustained HIV infection in CD34$^+$ cord blood cell-transplanted Rag2$^{-/-}\gamma_c^{-/-}$ mice. Proc. Natl. Acad. Sci. USA **103:**15951–15956.
4. **Berges, B. K., S. R. Akkina, J. M. Folkvord, E. Connick, and R. Akkina.** 2008. Mucosal transmission of R5 and X4 tropic HIV-1 via vaginal and rectal routes in humanized Rag2$^{-/-}$ $\gamma c^{-/-}$ (RAG-hu) mice. Virology **373:**342–351.
5. **Berges, B. K., W. H. Wheat, B. E. Palmer, E. Connick, and R. Akkina.** 2006. HIV-1 infection and CD4 T cell depletion in the humanized Rag2$^{-/-}$ $\gamma c^{-/-}$ (RAG-hu) mouse model. Retrovirology **3:**76.
6. **Blum, M. R., G. E. Chittick, J. A. Begley, and J. Zong.** 2007. Steady-state pharmacokinetics of emtricitabine and tenofovir disoproxil fumarate administered alone and in combination in healthy volunteers. J. Clin. Pharmacol. **47:**751–759.
7. **Denton, P. W., J. D. Estes, Z. Sun, F. A. Othieno, B. L. Wei, A. K. Wege, D. A. Powell, D. Payne, A. T. Haase, and J. V. Garcia.** 2008. Antiretroviral preexposure prophylaxis prevents vaginal transmission of HIV-1 in humanized BLT mice. PLoS Med. **5:**e16.
8. **Engelman, A., and R. Craigie.** 1992. Identification of conserved amino acid residues critical for human immunodeficiency virus type 1 integrase function in vitro. J. Virol. **66:**6361–6369.
9. **Gerton, J. L., S. Ohgi, M. Olsen, J. DeRisi, and P. O. Brown.** 1998. Effects of mutations in residues near the active site of human immunodeficiency virus type 1 integrase on specific enzyme-substrate interactions. J. Virol. **72:**5046–5055.
10. **Hammer, S. M., J. J. Eron, Jr., P. Reiss, R. T. Schooley, M. A. Thompson, S. Walmsley, P. Cahn, M. A. Fischl, J. M. Gatell, M. S. Hirsch, D. M. Jacobsen, J. S. Montaner, D. D. Richman, P. G. Yeni, and P. A. Volberding.** 2008. Antiretroviral treatment of adult HIV infection: 2008 recommendations of the International AIDS Society-USA panel. JAMA **300:**555–570.
11. **Miller, M., R. Danovich, S. Fransen, S. Gupta, W. Huang, Y. Ke, B. Nguyen, N. Parkin, C. Petropoulos, H. Teppler, M. Witmer, J. Zhao, and D. J. Hazuda.** 2008. Analysis of resistance to the HIV-1 integrase inhibitor raltegravir: results from the Benchmrk 1 and 2, abstr. H-898. Abstr. 48th Annu. Intersci. Conf. Antimicrob. Agents Chemother. (ICAAC)-Infect. Dis. Soc. Am. (IDSA) 46th Annu. Meet. American Society for Microbiology and Infectious Diseases Society of America, Washington, DC.
12. **Hazuda, D. J., P. Felock, M. Witmer, A. Wolfe, K. Stillmock, J. A. Grobler, A. Espeseth, L. Gabryelski, W. Schleif, C. Blau, and M. D. Miller.** 2000. Inhibitors of strand transfer that prevent integration and inhibit HIV-1 replication in cells. Science **287:**646–650.
13. **Hazuda, D. J., S. D. Young, J. P. Guare, N. J. Anthony, R. P. Gomez, J. S. Wai, J. P. Vacca, L. Handt, S. L. Motzel, H. J. Klein, G. Dornadula, R. M. Danovich, M. V. Witmer, K. A. Wilson, L. Tussey, W. A. Schleif, L. S. Gabryelski, L. Jin, M. D. Miller, D. R. Casimiro, E. A. Emini, and J. W. Shiver.** 2004. Integrase inhibitors and cellular immunity suppress retroviral replication in rhesus macaques. Science **305:**528–532.
14. **Hofer, U., S. Baenziger, M. Heikenwalder, E. Schlaepfer, N. Gehre, S. Regenass, T. Brunner, and R. F. Speck.** 2008. RAG2$^{-/-}\gamma_c^{-/-}$ mice transplanted with CD34$^+$ cells from human cord blood show low levels of intestinal engraftment and are resistant to rectal transmission of human immunodeficiency virus. J. Virol. **82:**12145–12153.
15. **Malet, I., O. Delelis, M.-A. Valantin, B. Montes, C. Soulie, M. Wirden, L. Tchertanov, G. Peytavin, J. Reynes, J.-F. Mouscadet, C. Katlama, V. Calvez, and A.-G. Marcelin.** 2008. Mutations associated with failure of raltegravir treatment affect integrase sensitivity to the inhibitor in vitro. Antimicrob. Agents Chemother. **52:**1351–1358.
16. **Margot, N. A., E. Isaacson, I. McGowan, A. K. Cheng, R. T. Schooley, and M. D. Miller.** 2002. Genotypic and phenotypic analyses of HIV-1 in antiretroviral-experienced patients treated with tenofovir DF. AIDS **16:**1227–1235.
17. **Markowitz, M., B. Y. Nguyen, E. Gotuzzo, F. Mendo, W. Ratanasuwan, C. Kovacs, G. Prada, J. O. Morales-Ramirez, C. S. Crumpacker, R. D. Isaacs, L. R. Gilde, H. Wan, M. D. Miller, L. A. Wenning, and H. Teppler.** 2007. Rapid and durable antiretroviral effect of the HIV-1 integrase inhibitor raltegravir as part of combination therapy in treatment-naive patients with HIV-1 infection: results of a 48-week controlled study. J. Acquir. Immune Defic. Syndr. **46:**125–133.
18. **North, T. W., K. K. Van Rompay, J. Higgins, T. B. Matthews, D. A. Wadford, N. C. Pedersen, and R. F. Schinazi.** 2005. Suppression of virus load by highly active antiretroviral therapy in rhesus macaques infected with a recombinant simian immunodeficiency virus containing reverse transcriptase from human immunodeficiency virus type 1. J. Virol. **79:**7349–7354.
19. **Rezk, N. L., R. D. Crutchley, and A. D. Kashuba.** 2005. Simultaneous quantification of emtricitabine and tenofovir in human plasma using high-performance liquid chromatography after solid phase extraction. J. Chromatogr. B Anal. Technol. Biomed. Life Sci. **822:**201–208.
20. **Stoddart, C. A., C. A. Bales, J. C. Bare, G. Chkhenkeli, S. A. Galkina, A. N. Kinkade, M. E. Moreno, J. M. Rivera, R. E. Ronquillo, B. Sloan, and P. L. Black.** 2007. Validation of the SCID-hu Thy/Liv mouse model with four classes of licensed antiretrovirals. PLoS ONE **2:**e655.
21. **Sun, Z., P. W. Denton, J. D. Estes, F. A. Othieno, B. L. Wei, A. K. Wege, M. W. Melkus, A. Padgett-Thomas, M. Zupancic, A. T. Haase, and J. V. Garcia.** 2007. Intrarectal transmission, systemic infection, and CD4+ T cell depletion in humanized mice infected with HIV-1. J. Exp. Med. **204:**705–714.
22. **Traggiai, E., L. Chicha, L. Mazzucchelli, L. Bronz, J. C. Piffaretti, A. Lanzavecchia, and M. G. Manz.** 2004. Development of a human adaptive immune system in cord blood cell-transplanted mice. Science **304:**104–107.
23. **Zhang, L., G. I. Kovalev, and L. Su.** 2007. HIV-1 infection and pathogenesis in a novel humanized mouse model. Blood **109:**2978–2981.